



Cite this: *J. Mater. Chem. A*, 2016, 4, 15370

## *In situ* large-scale construction of sulfur-functionalized metal–organic framework and its efficient removal of Hg(II) from water†

Linfeng Liang,<sup>abd</sup> Qihui Chen,<sup>\*ac</sup> Feilong Jiang,<sup>ac</sup> Daqiang Yuan,<sup>ac</sup> Jinjie Qian,<sup>a</sup> Guangxun Lv,<sup>a</sup> Hui Xue,<sup>ac</sup> Luyao Liu,<sup>a</sup> Hai-Long Jiang<sup>bd</sup> and Maochun Hong<sup>\*acd</sup>

A new strategy that uses sulfur-functionalized metal organic frameworks (MOFs) for removal of Hg(II) from water has been developed. This strategy is based around a novel sulfur-functionalized MOF FJI-H12, which is composed of octahedral  $M_6L_4$  cages and free  $NCS^-$  groups. At the same time, large-scale synthesis of FJI-H12 microcrystals has also been carried out under very mild conditions. The resulting material can remove Hg(II) completely and selectively from water with high saturation, adsorption ( $439.8\text{ mg g}^{-1}$ ) and distribution coefficient ( $1.85 \times 10^6\text{ mL g}^{-1}$ ) relative to other MOFs. More interestingly, a continuous and fast removal of Hg(II) from water has also been carried out using a column loaded with FJI-H12 microcrystals.

Received 13th June 2016  
Accepted 10th September 2016

DOI: 10.1039/c6ta04927c

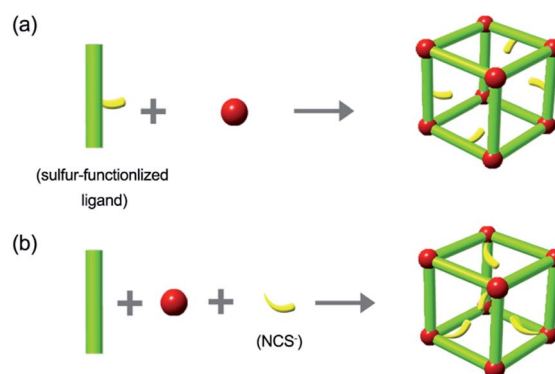
www.rsc.org/MaterialsA

### Introduction

Mercury (Hg) pollution, which can cause birth defects, brain damage, and various other diseases in humans and animals, has become a serious threat to public health and the environment. Hence, the development of methods for its removal from waste water is highly urgent.<sup>1</sup> A variety of adsorbents, such as activated carbons, zeolites and clays, have already been used for this purpose; however, such materials usually face challenges such as low surface area, low capacity, and moderate affinity for Hg(II).<sup>2</sup> Metal–organic frameworks (MOFs), based on organic bridging ligands and metal ions or metal ion clusters, are a promising class of highly ordered, porous materials that have potential applications in gas storage, catalysis, and drug delivery, due to their unique properties such as permanent porosity and high crystallinity.<sup>3</sup> Readily accessible external and internal surfaces and evenly distributed active sites through purposeful design make adsorption of heavy metal ions by MOFs possible.<sup>4</sup> Methylthio groups were first introduced into MOFs to adsorb Hg(II) by Xu and coworkers.<sup>5</sup> Many other functional groups have since been introduced to capture Hg(II)

based on Hg–S interactions or Hg–N interactions. Sulfur-functionalized MOFs based on strong Hg–S interaction have proved particularly useful as sorbents for Hg(II).<sup>6</sup>

The synthesis of sulfur-functionalized MOFs using preconstructed sulfur-functionalized ligands is illustrated in Scheme 1a. While this can be a powerful strategy for Hg(II) removal, it usually requires expensive reagents or harsh reaction conditions.<sup>7</sup> *In situ* introduction of sulfur-containing groups into MOFs based on coordination bonding might be an effective approach to overcome such challenges. The  $NCS^-$  group is an ideal candidate for this route; it could be introduced into the framework during MOFs construction by coordination of the chemically hard N atom to a hard metal ion, while the chemically soft S atom remains available for the capture of heavy metal ions such as Hg(II) (Scheme 1b). Although  $NCS^-$  has been



**Scheme 1** (a) The construction of sulfur-functionalized MOFs based on pre-designed sulfur-functionalized ligands. (b) *In situ* introduction of sulfur-containing groups into MOFs based on coordination bonds.

<sup>a</sup>State Key Lab of Structure Chemistry, Fujian Institute of Research on the Structure of Matter, Chinese Academy of Sciences, Fuzhou, 350002, Fujian, China. E-mail: chengh@fjirm.ac.cn; hmc@fjirm.ac.cn

<sup>b</sup>Department of Chemistry, Hefei National Laboratory for Physical Sciences at the Microscale, Hefei, Anhui 230026, P. R. China

<sup>c</sup>University of the Chinese Academy of Sciences, Beijing, 100049, China

<sup>d</sup>Department of Chemistry, University of Science and Technology of China, Hefei, Anhui 230026, P. R. China

† Electronic supplementary information (ESI) available. CCDC 1474064. For ESI and crystallographic data in CIF or other electronic format see DOI: 10.1039/c6ta04927c

used to construct discrete metallocages or MOFs,<sup>8</sup> as far as we know, use of such material to capture Hg(II) has not been reported. Herein, a novel sulfur-functionalized MOF **FJI-H12** was constructed using NCS<sup>−</sup>, Co(II) and 2,4,6-tri(1-imidazolyl)-1,3,5-triazine (Timt). The components were arranged in infinite octahedral M<sub>6</sub>L<sub>4</sub> cages containing free NCS<sup>−</sup> groups. As we expected, N atoms of NCS<sup>−</sup> are coordinated to Co atoms, while the S atoms are free-standing. Moreover, large-scale synthesis of **FJI-H12** microcrystals has also been realized under very mild conditions. Further researches demonstrate that such a material can remove Hg(II) from water completely and selectively. More interestingly, a continuous and fast removal of Hg(II) from water has been realized using a column loaded with **FJI-H12** microcrystals.

## Results and discussion

### Syntheses and structures of FJI-H12

Layering an ethanol solution of Timt onto a water solution of K<sub>2</sub>Co(NCS)<sub>4</sub> at room temperature for three days leads to the formation of light pink octahedral single crystals (denoted as **FJI-H12**), formulated as [Co<sub>3</sub>(Timt)<sub>4</sub>(SCN)<sub>6</sub>(H<sub>2</sub>O)<sub>14</sub>(EtOH)]<sub>n</sub> (for details, please refer to ESI S1†). Single crystal X-ray analysis reveals that **FJI-H12** has a two-fold penetration structure and each fold comprises an infinite array of octahedral M<sub>6</sub>L<sub>4</sub> cages, which are constructed by six Co(II) vertexes and four Timt panels (Fig. 1a and b). Apart from four imidazole rings, each Co(II) vertex of the M<sub>6</sub>L<sub>4</sub> cage also bonds to two NCS<sup>−</sup> groups at their chemically hard N-sides, leaving their chemically soft S atoms pointing into the cavity (Fig. 1c).

### Metal ions selective adsorption test of FJI-H12

Although there is a two-fold penetration, **FJI-H12** is still highly porous and this can be confirmed by single component low-pressure gas adsorption test. N<sub>2</sub> adsorption isotherms at 77.4 K revealed its microporous nature (Fig. S1†). The pore size distribution ranges from 6.8 Å to 14.9 Å (Fig. S2†), which is far larger than the Hg(II) ion radius and obviously can guarantee the accessibility of free-standing S atoms for Hg(II) adsorption. Before metal adsorption testing, the chemical stability in various reagents and the thermal stability of **FJI-H12** were investigated. We ultimately found that **FJI-H12** is stable in water and various organic solvents, such as acetone, methanol, isopropanol, cyclohexane and ethanol (Fig. S3†), and it is thermally stable up to 200 °C (Fig. S4†).

The metal selectivity tests were firstly performed on **FJI-H12** in a 50 mL Hg(II) solution containing Mn(II), Ba(II), Ni(II), and Cd(II) background ions in high concentrations. Not only did **FJI-H12** completely remove Hg(II) from the test sample, after which Hg(II) was not detected by ICP, but it also absorbed another highly toxic heavy metal ion, Cd(II). In contrast, other background metal ions, Mn(II), Ba(II) and Ni(II), were not adsorbed by **FJI-H12** in a significant quantity (Table 1). The high selectivity of **FJI-H12** for Hg(II) relative to the other metal ions such as Cd(II), Mn(II), Ba(II), and Ni(II) observed for **FJI-H12** may result from the strong Hg–S interactions, which have been demonstrated by FT-IR studies. As shown in Fig. 2, the typical stretch mode of SCN<sup>−</sup>

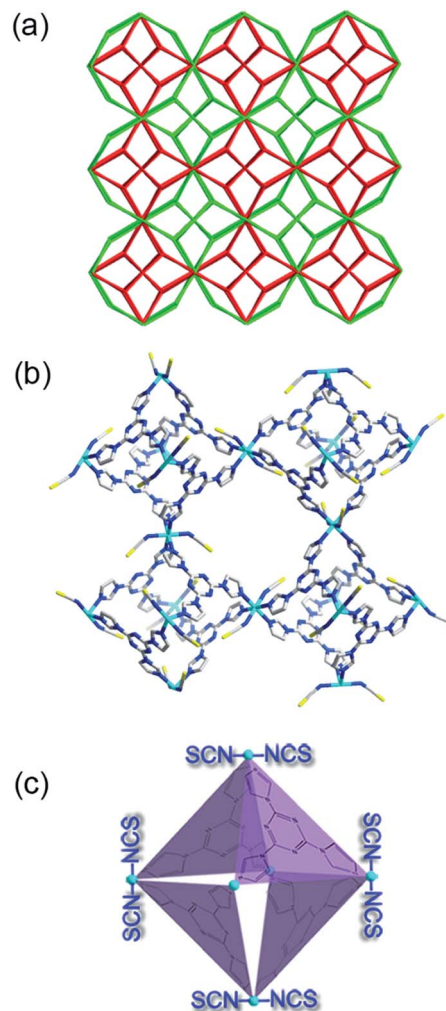


Fig. 1 (a) The topological structure of **FJI-H12** with a two-fold penetration. (b) Stick model of one-fold network composed of M<sub>6</sub>L<sub>4</sub> cages (C = grey, N = light blue, S = yellow, Co = cyan and H was omitted for clarity). (c) Schematic of one M<sub>6</sub>L<sub>4</sub> cage with coordinated NCS<sup>−</sup> groups.

shows a large shift from 2072 cm<sup>−1</sup> to 2125 cm<sup>−1</sup> in **FJI-H12**–Hg (the **FJI-H12** sample after Hg adsorption), indicating the strong binding interactions between Hg(II) and SCN<sup>−</sup>.

### Hg(II) saturation adsorption amount of FJI-H12

To assess the mercury adsorption capacity of **FJI-H12**, which is also an important aspect of a sorbent's performance, an

Table 1 Concentrations (ppm) of metal ions before and after treatment of **FJI-H12**

Metal ion	Hg	Cd	Ni	Ba	Mn
Before treatment	20.45	84.82	128.89	107.71	126.68
After treatment <sup>a</sup>	— <sup>b</sup>	58.53	128.82	106.77	126.24

<sup>a</sup> Treatment conditions: excess **FJI-H12** (200 mg) was added to 50 mL water solution of metal ions and stirred at room temperature for 12 hours. The concentration of each metal is determined before and after treatment by Inductively Coupled Plasma (ICP). <sup>b</sup> The real value is less than the limit of detection of ICP instrument (0.02 ppb).



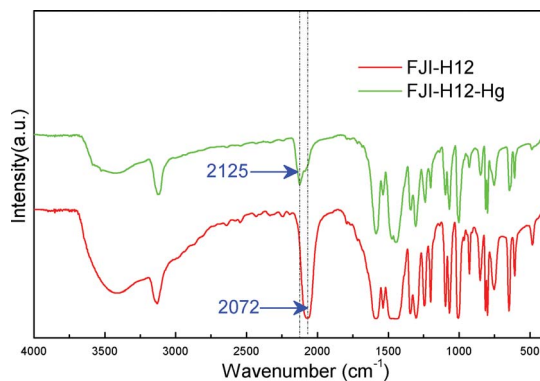


Fig. 2 FT-IR spectra of FJI-H12 (red) and FJI-H12-Hg (green).

activated sample of **FJI-H12** (100 mg) and 50 mL aqueous  $\text{HgCl}_2$  solution (397 mg  $\text{HgCl}_2$ , 4 equivalents) were stirred together at room temperature for 12 h. The solid was then isolated by centrifugation and further washed with ethanol/ $\text{H}_2\text{O}$  to remove residual  $\text{HgCl}_2$  on the exterior of the **FJI-H12** powder sample. The solid sample thus obtained was subjected to regular inductively coupled plasma (ICP) analysis. Testing determined the  $\text{Hg}/\text{Co}$  ratio to be 1.20/1, corresponding to a maximum mercury adsorption capacity  $q_{\text{max}}$  of  $439.8 \text{ mg g}^{-1}$  ( $2.19 \text{ mmol g}^{-1}$ ), a value which is very high relative to other MOF materials (Table 2). Further researches over the pH range of 3.0 to 6.0 demonstrate that **FJI-H12** shows its highest adsorption capacity at pH = 7; when the pH is increased from 3.0 to 6.0, the removal efficiency capacity is basically unchanged (Fig. S5†).

### Hg(II) adsorption kinetics

Given the high  $\text{Hg(II)}$  saturation level of this material, another test that focuses on its kinetic character has been carried out as follows: an activated **FJI-H12** sample (10 mg) was placed in a dilute aqueous solution (50 mL) of  $\text{HgCl}_2$  (10 ppm). The residual  $\text{Hg(II)}$  concentration in the solution was determined at different intervals. Fig. 3a shows the fitting results of the experimental data for mercury adsorption on **FJI-H12** by the pseudo-second-order kinetic model using the following equation:

Table 2 Comparison of maximum mercury adsorption capacity  $q_{\text{max}}$  (ppm) and  $K_d$  value ( $\text{mL g}^{-1}$ ) of **FJI-H12** with other MOFs materials

MOF	$q_{\text{max}}, \text{mg g}^{-1}$	$K_d, \text{mL g}^{-1}$	Ref.
Pb-TMBD	361.3 <sup>a</sup>	—	5
Zr-DMBD	198.2	$9.99 \times 10^5$	6e
Zn-hip	278	$1.11 \times 10^6$	6d
PCN-100	364.7 <sup>b</sup>	—	6a
PCN-101	103.9 <sup>b</sup>	—	6a
$\text{Zn}_4\text{O(L)}_3$	102.8 <sup>c</sup>	$3.16 \times 10^3$	6b
<b>FJI-H12</b>	439.8	$1.86 \times 10^6$	This work

<sup>a</sup> The adsorption of  $\text{Hg(II)}$  from benzene. <sup>b</sup> The adsorption of  $\text{Hg(II)}$  from DMF. <sup>c</sup> The adsorption of  $\text{Hg(II)}$  from ethanol and the rest were processed in water.

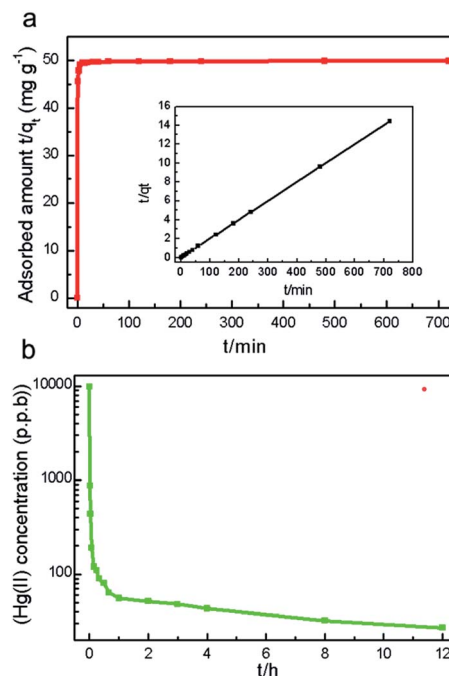


Fig. 3 (a)  $\text{Hg(II)}$  sorption kinetics of **FJI-H12** under initial  $\text{Hg(II)}$  concentration of 10 ppm. (b) Adsorption amount curve of  $\text{Hg(II)}$  versus contact time in an aqueous solution using **FJI-H12**. Inset shows the pseudo-second-order kinetic plot for the adsorption ( $\text{Hg(II)}$  concentration: 10 ppm).

$$\frac{t}{q_t} = \frac{1}{k_2 q_e^2} + \frac{t}{q_e}$$

where  $q_t$  ( $\text{mg g}^{-1}$ ) and  $q_e$  ( $\text{mg g}^{-1}$ ) are the  $\text{Hg(II)}$  adsorption amounts at time  $t$  (min) and at equilibrium, respectively, and  $k_2$  ( $\text{g mg}^{-1} \text{min}^{-1}$ ) is the rate constant of pseudo-second order adsorption. An extremely high correlation coefficient ( $>0.9999$ ) was obtained (Fig. 3b and the inset), suggesting that the pseudo-second-order model is suitable for describing the adsorption kinetics of this system. Furthermore, the calculated  $q_e$  value from the pseudo-second-order model is in good agreement with the experimental value,  $q_{e,\text{exp}}$  (Table S2†). Consequently, it is believed that mechanisms of both physisorption and chemisorption are involved in the current  $\text{Hg(II)}$  adsorption process, although to different degrees. Specifically, the  $\text{SCN}^-$  groups in the pores hold the potential to coordinate with  $\text{Hg(II)}$  ions, and act as strong sites for  $\text{Hg(II)}$  chemisorptions.

The distribution coefficient ( $K_d$ ) is always used to characterize a sorbent's affinity for a target metal ion, which is defined as follows:

$$K_d = \frac{(C_i - C_f)}{C_f} \times \frac{V}{m}$$

where  $C_i$  and  $C_f$  are the initial metal ion concentration and the final equilibrium metal ion concentration, respectively,  $V$  (mL) is the volume of the treated solution and  $m$  (g) is the mass of sorbent used.  $K_d$  values of  $1.0 \times 10^5 \text{ mL g}^{-1}$  are usually considered excellent;<sup>9</sup> the  $K_d$  of **FJI-H12** for  $\text{Hg(II)}$  is an exceptional  $1.85 \times 10^6 \text{ mL g}^{-1}$ . As far as we know, this value is among



the highest for MOF materials for Hg(II) adsorption reported thus far (Table 2). This exceptional  $K_d$  value can be ascribed to the large pore size of **FJI-H12**, which facilitates the diffusion of Hg(II) ions, and its high surface area that is densely populated with  $\text{SCN}^-$  groups, which have strong interactions with Hg(II) ions.

### Regeneration of FJI-H12

Whether an adsorbent can be regenerated is also an important aspect of its usefulness. To this point, a KSCN solution was used to regenerate a **FJI-H12-Hg** sample. By immersing **FJI-H12-Hg** in the KSCN solution (10 equivalents) at ambient temperature for 1 day, over 86% of the Hg(II) ions could be removed from **FJI-H12-Hg** powder (ICP analysis determined the Hg/Co ratio drops from 1.20/1 to 0.17/1 during this process), while the framework of **FJI-H12** remains stable (Fig. S6†). Reuse of the regenerated **FJI-H12** sample under the same conditions resulted in the corresponding Hg/Co ratio being reduced to 0.86/1, indicating that the efficiency of **FJI-H12** is highly reduced after regeneration.

### Large-scale synthesis of FJI-H12 and continuous removal of Hg

Several excellent sorbents based on strong Hg-S interactions have been developed; however, large-scale preparation and application of such materials are still highly challenging.<sup>6,10</sup> After many attempts, a protocol for large-scale preparation of **FJI-H12** has been established as follows: a high concentration water solution (1 mol L<sup>-1</sup>, 0.3 mL) of  $\text{K}_2\text{Co}(\text{SCN})_4$  was added to a vigorously stirred ethanol solution (0.02 mol L<sup>-1</sup>, 20 mL) of Tmt, immediately leading to the formation of a uniform

microcrystalline powder of **FJI-H12**. Its purity has been confirmed by powder X-ray diffraction (PXRD) analysis (Fig. 4a). The median microcrystal grain size was determined by laser diffraction analysis to be  $X_{50} = 2.1 \mu\text{m}$  (Fig. S7†). Scanning electron microscopy measurements also confirmed the formation of relatively uniform octahedral crystallites on the scale of about 2  $\mu\text{m}$  (Fig. S8†). Moreover, the observed crystalline morphology is in accordance with the large single crystal obtained by the solution diffusion method (Fig. 4b and the inset). Further researches indicated that up to 10 g **FJI-H12** could be prepared by this method (Fig. S6†).

Since large-scale synthesis of **FJI-H12** has been realized under very mild conditions, this makes possible the removal of Hg(II) from water on a large scale. A column for removal of Hg(II) from water was prepared by loading 2 g of **FJI-H12** microcrystal powder into a 10 mL syringe equipped with a 0.22  $\mu\text{m}$  Millipore filter (schematic in Fig. 4c). A 20 ppm Hg solution in 50 mL water could be completely purified by this column at a flow rate of 2 mL min<sup>-1</sup>. This represents the first continuous and fast removal of Hg(II) from water based on sulfur-functionalized MOF. It also implies the practicality of such materials for the waste-water treatment in industry.

## Conclusions

In conclusion, a novel sulfur-functionalized metal-organic framework **FJI-H12** has been synthesized for the capture of Hg(II) from water. Moreover, its microcrystalline powder can be synthesized up to 10 g scale within several minutes under very mild condition. Such material can remove Hg(II) completely and selectively from water with high saturation (439.8 mg g<sup>-1</sup>) and distribution coefficient ( $1.85 \times 10^6 \text{ mL g}^{-1}$ ) as compared to other MOF materials. More interestingly, a continuous and fast removal of Hg(II) from water has also been carried out using a column loaded with **FJI-H12** microcrystalline powder. Thus, *in situ* construction of sulfur-functionalized MOF based on the  $\text{SCN}^-$  group provides a new perspective for decontaminating Hg(II) from aqueous media and makes both large-scale synthesis and application of sulfur-functionalized MOF for Hg(II) capture more practical.

## Acknowledgements

We are thankful for financial support from the 973 Program (2014CB932101, 2013CB933200), the "Strategic Priority Research Program" of the Chinese Academy of Sciences (XDA09030102, XDA07070200), and the National Natural Science Foundation of China (21471148, 21131006).

## Notes and references

- (a) N. Lubick and D. Malakoff, *Science*, 2013, **341**, 1443–1445; (b) M. McNutt, *Science*, 2013, **341**, 1430; (c) C. Wang, S. Tao, W. Wei, C. Meng, F. Liu and M. Han, *J. Mater. Chem.*, 2010, **20**, 4635–4641.
- (a) U. Wingenfelder, C. Hansen, G. Furrer and R. Schulin, *Environ. Sci. Technol.*, 2005, **39**, 4606–4613; (b)

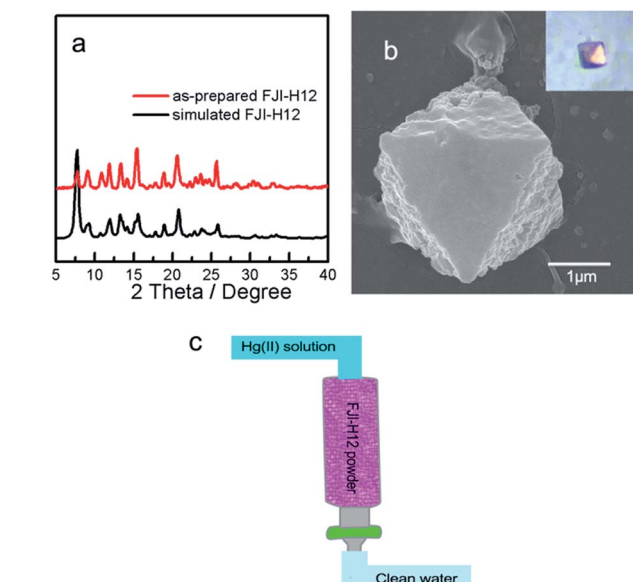


Fig. 4 (a) PXRD patterns of FJI-H12 from simulated FJI-H12 (black) and the as-synthesized sample (red). (b) Morphology comparison between SEM images of FJI-H12 microcrystal and single crystal (inset). (c) Schematic of separation column packed with FJI-H12 microcrystals.





- A. Benhammou, A. Yaacoubi, L. Nibou and B. Tanouti, *J. Colloid Interface Sci.*, 2005, **282**, 320–326; (c) G. Blanchard, M. Maunaye and G. Martin, *Water Res.*, 1984, **18**, 1501–1507; (d) C. P. Huang and D. W. Blankenship, *Water Res.*, 1984, **18**, 37–46.
- 3 (a) B. Li, M. Chrzanowski, Y. Zhang and S. Ma, *Coord. Chem. Rev.*, 2016, **307**, 106–129, part 2; (b) L. Ma, C. Abney and W. Lin, *Chem. Soc. Rev.*, 2009, **38**, 1248–1256; (c) J.-P. Zhang, Y.-B. Zhang, J.-B. Lin and X.-M. Chen, *Chem. Rev.*, 2012, **112**, 1001–1033; (d) Y. Cui, Y. Yue, G. Qian and B. Chen, *Chem. Rev.*, 2012, **112**, 1126–1162; (e) D. Zhao, D. J. Timmons, D. Yuan and H.-C. Zhou, *Acc. Chem. Res.*, 2011, **44**, 123–133; (f) P. Silva, S. M. F. Vilela, J. P. C. Tome and F. A. Almeida Paz, *Chem. Soc. Rev.*, 2015, **44**, 6774–6803; (g) Q. Yang, D. Liu, C. Zhong and J.-R. Li, *Chem. Rev.*, 2013, **113**, 8261–8323; (h) S. M. Cohen, *Chem. Rev.*, 2012, **112**, 970–1000; (i) J. Lee, O. K. Farha, J. Roberts, K. A. Scheidt, S. T. Nguyen and J. T. Hupp, *Chem. Soc. Rev.*, 2009, **38**, 1450–1459; (j) P. Horcajada, R. Gref, T. Baati, P. K. Allan, G. Maurin, P. Couvreur, G. Férey, R. E. Morris and C. Serre, *Chem. Rev.*, 2012, **112**, 1232–1268; (k) R. C. Huxford, J. Della Rocca and W. Lin, *Curr. Opin. Chem. Biol.*, 2010, **14**, 262–268; (l) M. Eddaoudi, D. F. Sava, J. F. Eubank, K. Adil and V. Guillermin, *Chem. Soc. Rev.*, 2015, **44**, 228–249; (m) J. J. I. V. Perry, J. A. Perman and M. J. Zaworotko, *Chem. Soc. Rev.*, 2009, **38**, 1400–1417; (n) M. O’Keeffe and O. M. Yaghi, *Chem. Rev.*, 2012, **112**, 675–702; (o) M. P. Suh, H. J. Park, T. K. Prasad and D.-W. Lim, *Chem. Rev.*, 2012, **112**, 782–835; (p) H. Wu, Q. Gong, D. H. Olson and J. Li, *Chem. Rev.*, 2012, **112**, 836–868; (q) T. Uemura, N. Yanai and S. Kitagawa, *Chem. Soc. Rev.*, 2009, **38**, 1228–1236; (r) K. Sumida, D. L. Rogow, J. A. Mason, T. M. McDonald, E. D. Bloch, Z. R. Herm, T.-H. Bae and J. R. Long, *Chem. Rev.*, 2012, **112**, 724–781; (s) A. Dhakshinamoorthy, A. M. Asiri and H. Garcia, *Chem. Soc. Rev.*, 2015, **44**, 1922–1947; (t) Y. Yan, S. Yang, A. J. Blake and M. Schroeder, *Acc. Chem. Res.*, 2014, **47**, 296–307; (u) K. Sumida, D. L. Rogow, J. A. Mason, T. M. McDonald, E. D. Bloch, Z. R. Herm, T.-H. Bae and J. R. Long, *Chem. Rev.*, 2012, **112**, 724–781; (v) S. S. Han, J. L. Mendoza-Cortes and W. A. Goddard III, *Chem. Soc. Rev.*, 2009, **38**, 1460–1476.
- 4 (a) M. Carboni, C. W. Abney, S. Liu and W. Lin, *Chem. Sci.*, 2013, **4**, 2396–2402; (b) J. Cui, Y. L. Wong, M. Zeller, A. D. Hunter and Z. Xu, *Angew. Chem., Int. Ed.*, 2014, **53**, 14438–14442; (c) J. He, M. Zha, J. Cui, M. Zeller, A. D. Hunter, S.-M. Yiu, S.-T. Lee and Z. Xu, *J. Am. Chem. Soc.*, 2013, **135**, 7807–7810; (d) M. Zha, J. Liu, Y.-L. Wong and Z. Xu, *J. Mater. Chem. A*, 2015, **3**, 3928–3934; (e) Y. Wang, G. Ye, H. Chen, X. Hu, Z. Niu and S. Ma, *J. Mater. Chem. A*, 2015, **3**, 15292–15298; (f) Y. Wang, Z. Liu, Y. Li, Z. Bai, W. Liu, Y. Wang, X. Xu, C. Xiao, D. Sheng, J. Diwu, J. Su, Z. Chai, T. E. Albrecht-Schmitt and S. Wang, *J. Am. Chem. Soc.*, 2015, **137**, 6144–6147; (g) X. Meng, R.-L. Zhong, X.-Z. Song, S.-Y. Song, Z.-M. Hao, M. Zhu, S.-N. Zhao and H.-J. Zhang, *Chem. Commun.*, 2014, **50**, 6406–6408; (h) H. Xue, Q. Chen, F. Jiang, D. Yuan, G. Lv, L. Liang, L. Liu and M. Hong, *Chem. Sci.*, 2016, **7**, 5983–5988.
- 5 X. P. Zhou, Z. Xu, M. Zeller and A. D. Hunter, *Chem. Commun.*, 2009, 5439–5441.
- 6 (a) Q. R. Fang, D. Q. Yuan, J. Sculley, J. R. Li, Z. B. Han and H. C. Zhou, *Inorg. Chem.*, 2010, **49**, 11637–11642; (b) J. He, K.-K. Yee, Z. Xu, M. Zeller, A. D. Hunter, S. S.-Y. Chui and C.-M. Che, *Chem. Mater.*, 2011, **23**, 2940–2947; (c) T. Liu, J. X. Che, Y. Z. Hu, X. W. Dong, X. Y. Liu and C. M. Che, *Chem.–Eur. J.*, 2014, **20**, 14090–14095; (d) F. Luo, J. L. Chen, L. L. Dang, W. N. Zhou, H. L. Lin, J. Q. Li, S. J. Liu and M. B. Luo, *J. Mater. Chem. A*, 2015, **3**, 9616–9620; (e) K. K. Yee, N. Reimer, J. Liu, S. Y. Cheng, S. M. Yiu, J. Weber, N. Stock and Z. Xu, *J. Am. Chem. Soc.*, 2013, **135**, 7795–7798.
- 7 (a) S. V. Ley and A. W. Thomas, *Angew. Chem., Int. Ed.*, 2003, **42**, 5400–5449; (b) T. Kondo and T.-A. Mitsudo, *Chem. Rev.*, 2000, **100**, 3205–3220; (c) L. Vial, R. F. Ludlow, J. Leclaire, R. Pérez-Fernández and S. Otto, *J. Am. Chem. Soc.*, 2006, **128**, 10253–10257.
- 8 (a) M. B. Duriska, S. M. Neville, J. Lu, S. S. Iremonger, J. F. Boas, C. J. Kepert and S. R. Batten, *Angew. Chem., Int. Ed.*, 2009, **48**, 8919–8922; (b) S. M. Neville, B. Moubaraki, K. S. Murray and C. J. Kepert, *Angew. Chem., Int. Ed.*, 2007, **46**, 2059–2062; (c) Y. Inokuma, T. Arai and M. Fujita, *Nat. Chem.*, 2010, **2**, 780–783.
- 9 Y. Shin, G. E. Fryxell, W. Um, K. Parker, S. V. Mattigod and R. Skaggs, *Adv. Funct. Mater.*, 2007, **17**, 2897–2901.
- 10 (a) S.-Y. Ding, M. Dong, Y.-W. Wang, Y.-T. Chen, H.-Z. Wang, C.-Y. Su and W. Wang, *J. Am. Chem. Soc.*, 2016, **138**, 3031–3037; (b) B. Li, Y. Zhang, D. Ma, Z. Shi and S. Ma, *Nat. Commun.*, 2014, **5**, 5537.

